SCIENTIFIC REPORTS

OPEN

SUBJECT AREAS:
ISCHAEMIA
CELL SIGNALLING
MEDICAL RESEARCH

Received
30 September 2014

Accepted
24 December 2014

Published
23 January 2015

Correspondence and requests for materials should be addressed to A.L. (alain.lacampagne@inserm.fr)

Activation of Sonic hedgehog signaling in ventricular cardiomyocytes exerts cardioprotection against ischemia reperfusion injuries

Ludovit Paulis[1], Jeremy Fauconnier[1], Olivier Cazorla[1], Jérome Thireau[1], Raffaella Soleti[2], Bastien Vidal[1], Aude Ouillé[1], Marion Bartholome[1], Patrice Bideaux[1], François Roubille[1], Jean-Yves Le Guennec[1], Ramaroson Andriantsitohaina[2], M. Carmen Martínez[2] & Alain Lacampagne[1]

[1]UMR CNRS 9214, Inserm U1046, Université de Montpellier, CHRU Montpellier, Montpellier, France, [2]INSERM U1063, Stress oxydant et pathologies métaboliques, LUNAM Université, Angers, France.

Sonic hedgehog (SHH) is a conserved protein involved in embryonic tissue patterning and development. SHH signaling has been reported as a cardio-protective pathway *via* muscle repair–associated angiogenesis. The goal of this study was to investigate the role of SHH signaling pathway in the adult myocardium in physiological situation and after ischemia-reperfusion. We show in a rat model of ischemia-reperfusion that stimulation of SHH pathway, either by a recombinant peptide or shed membranes microparticles harboring SHH ligand, prior to reperfusion reduces both infarct size and subsequent arrhythmias by preventing ventricular repolarization abnormalities. We further demonstrate in healthy animals a reduction of QTc interval mediated by NO/cGMP pathway leading to the shortening of ventricular cardiomyocytes action potential duration due to the activation of an inward rectifying potassium current sharing pharmacological and electrophysiological properties with ATP-dependent potassium current. Besides its effect on both angiogenesis and endothelial dysfunction we demonstrate here a novel cardio-protective effect of SHH acting directly on the cardiomyocytes. This emphasizes the pleotropic effect of SHH pathway as a potential cardiac therapeutic target.

The Hedgehog protein family is involved in early embryonic patterning and development especially of the neural tube in vertebrates[1]. Among the three proteins of the Hedgehog family, Sonic hedgehog homolog (SHH) plays a key role in regulating morphogenesis, organogenesis and left-right asymmetry[2]. In post-embryonic states and adult tissues, Hedgehog signaling is involved both in physiological and pathological processes. SHH signaling promotes neovascularization during ischemic diseases and appears as a promising candidate in cardioprotection settings[3,4]. In adult cardiovascular system, SHH participates in the maintenance of the coronary vasculature[5] and promotes angiogenesis[6] in mice, which could explain part of the cardioprotective effect of erythropoietin in a murine model of ischemia-reperfusion (IR)[7]. But the functional contribution of SHH signaling in adult cardiomyocytes remains unknown.

We have previously reported that shed membrane microparticles (MPs) derived from activated/apoptotic T lymphocytes harbor SHH (MPs^{SHH+}), trigger nitric oxide (NO) release from endothelial cells and correct severe endothelial injury[8–10]. These effects are prevented when SHH pathway is blocked, suggesting that MPs^{SHH+} exert some of their effects by triggering SHH signaling. Two transmembrane proteins Patched (Ptc) and Smoothened (Smo) have been identified as the receptor complex[11,12]. Ptc functions as Hedgehog-binding protein while Smo is required to transduce the signal. In the absence of SHH signal, Ptc inhibits the activity of Smo. When SHH binds to Ptc, Ptc is internalized and Smo inhibition is removed[12]. SHH has been reported to activate several intracellular pathways, including the phosphatidylinositol 3-kinase (PI3-K)/Akt pathway[13], which is associated with enhanced NO production in endothelial cells[14] and is a well-known mediator of cardioprotection in IR models.

The aim of this work was to investigate the impact of SHH pathway activation on cardiomyocytes in normal conditions and in a context of IR both *in vivo* and *in vitro* at the cardiomyocyte level. We show for the first time that activation of SHH pathway either by a recombinant SHH protein (N-SHH) or by MPs^{SHH+} offers a protection of the heart to IR by modulating cardiomyocyte electrophysiological properties.

Results

Effect of SHH on electrocardiogram in healthy animals. Electrocardiogram (ECG) analysis was performed on control vigil animals (Figure 1, S1) to evaluate ventricular repolarization over 6 hours of recording. In control conditions (Figure 1A, B), QT interval remained stable while 6 hours after the recombinant SHH homolog ligand (N-SHH) injection, a significant shortening occurred (Figure 1A, B). This was mimicked by a treatment with specific shed membrane MPs harboring SHH protein (MPs^{SHH+}) (Figure 1A, B). The N-SHH-induced effect was not modified when the animals were pre-treated with hexamethonium (Figure 1B, S1). Hexamethonium is a nicotinic (nACh) receptor antagonist that acts at pre-ganglionic sites in both the sympathetic and parasympathetic nervous systems and therefore inhibits cardiac regulation by autonomic nervous system. This strongly supports a direct myocardial effect of SHH independently of the autonomic system, and suggests an effect on cardiomyocyte action potential. In addition, simultaneous treatment with N-SHH and the SHH receptor (Ptc/Smo) antagonist cyclopamine prevented the changes in QT duration induced by N-SHH (Figure 1B, S1) demonstrating Smo activation in healthy control animals. However,

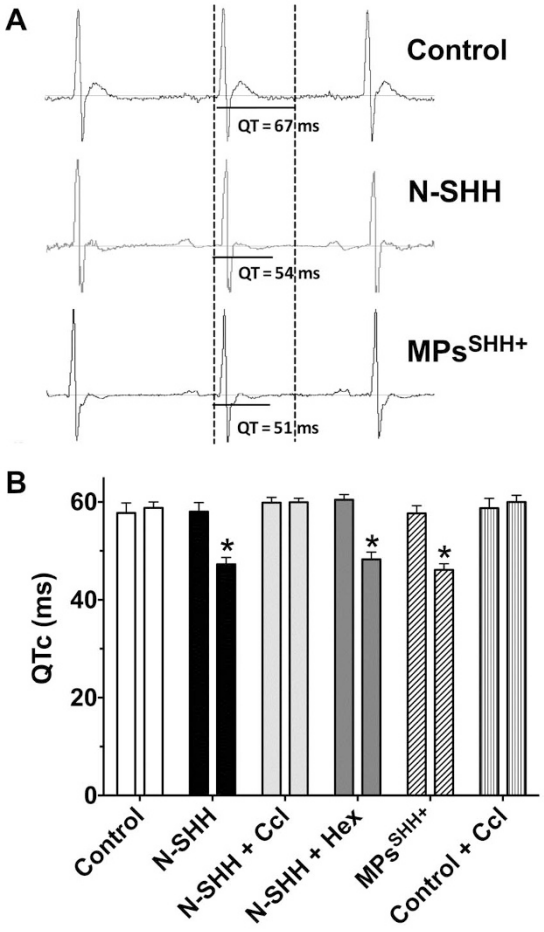

Figure 1 | Activation of SHH signaling shortens QT interval in healthy animals. (A) ECGs were acquired over 6 hours after different treatments (*i.p.*-injected), in control animals. Representative ECGs recorded in control, N-SHH- and MPs^{SHH+}-treated animals indicate a shortening of QT interval after SHH signaling pathway activation. (B) Mean QTc values recorded before (t = 0, left column) and 6 hours after injection (t = 6, right column) of the vehicle (control, n = 5), N-SHH (n = 8), N-SHH+Hexamethonium (N-SHH+Hex, n = 6), MPs^{SHH+} (n = 7), N-SHH and cyclopamine (N-SHH+Ccl, n = 6) and cyclopamine alone (Control + Ccl, n = 6). (* $p < 0.05$, QTc at 6 h *vs* t = 0).

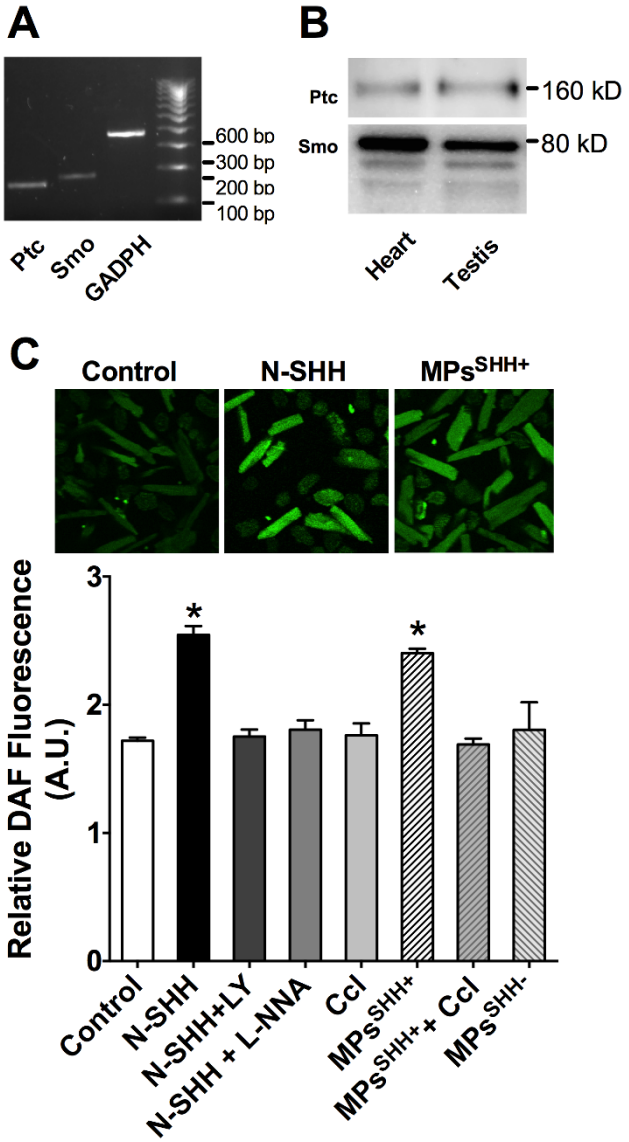

Figure 2 | SHH mediates NO production in ventricular cardiomyocytes. (A) Representative PCR gel showing the expression of Patched (Ptc) and Smoothened (Smo) and reference Glyceraldehyde 3-phosphate dehydrogenase (GAPDH) mRNAs in rat cardiomyocytes. (B) Smo and Ptc expression was revealed by Western blotting in cardiomyocytes and in testis used as reference tissue. These representative images correspond to extracted portion of membranes after transfer of the same gel and exposed respectively with anti- Smo and Ptc primary antibodies. Each band corresponds to adjacent wells of the gel. (C) Representative confocal images illustrating the increase in NO production after incubation of control cardiomyocytes with the recombinant SHH protein (N-SHH) or microparticles harboring the SHH protein (MPs^{SHH+}) for 4 h (upper panel). DAF fluorescence level (lower panel) was quantified in control (n = 495 cells), after incubation with N-SHH (n = 365 cells), and after co-incubation with phosphoinositide-3 kinase inhibitor, LY294002 (LY, 25 μM, n = 98 cells), NOS inhibitor, N^{Ω}-nitro-L-arginine (L-NNA, 100 μM, n = 98 cells). DAF fluorescence level was also quantified after incubation with MPs^{SHH+} (n = 382 cells) and after co-incubation with the SHH pathway inhibitor cyclopamine (MPs^{SHH+}-Ccl, 30 μM, n = 137 cells). Cyclopamine alone had no effect on basal levels of NO (Ccl, 30 μM, n = 68 cells). Incubation with MPs not carrying the SHH (MPs^{SHH-}) did not enhance NO formation (n = 23 cells). Data are mean ± SEM; *, $p < 0.05$ compared to control.

cyclopamine alone had no effect on ECG properties suggesting that SHH signaling was silent in basal conditions.

SHH pathway is present and functional in adult cardiomyocytes. Ptc and Smo were expressed in adult cardiomyocytes both at the mRNA (Figure 2A) and at the protein levels (Figure 2B). Considering that MPs^{SHH+} trigger NO release from endothelial cells[8–10], we tested the functionality of SHH pathway in adult cardiomyocytes loaded with the NO fluorescent probe DAF and incubated with the N-SHH (20 μM) for 4 hours (Figure 2C). When compared to non-treated cells, DAF fluorescence was significantly increased after N-SHH or MPs^{SHH+} incubation

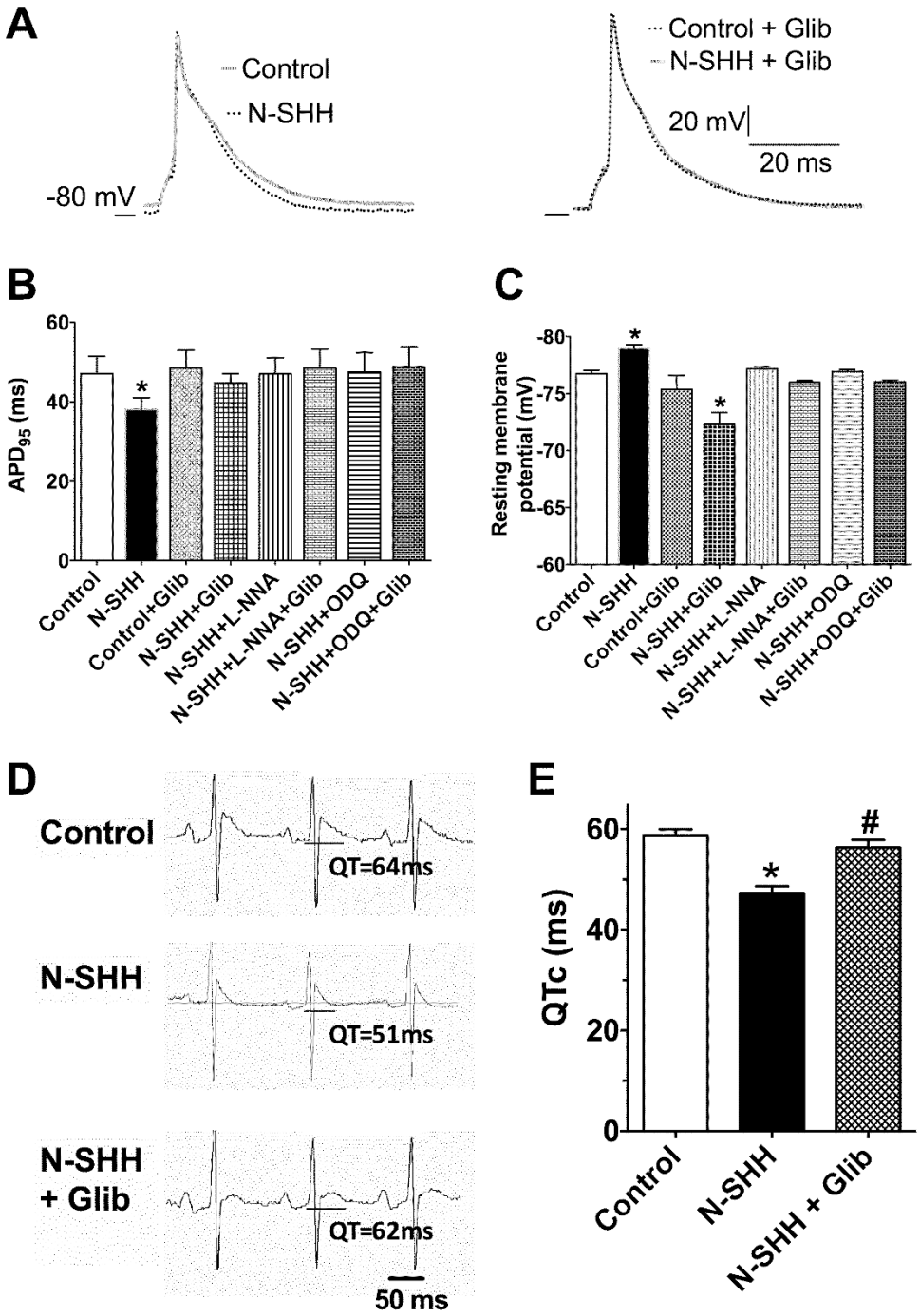

Figure 3 | SHH reduces action potential duration. (A) Representative traces of action potential recorded in control and after SHH treatment (left panel) and in the presence the ATP-dependent potassium channel inhibitor glibenclamide (1 μM) (right panel). (B) Average values of resting membrane potential in control (n = 7), SHH (n = 8), Control+glibenclamide (n = 7), N-SHH+glibenclamide (n = 8), N-SHH+L-NNA (n = 7), N-SHH+L-NNA+glibenclamide (n = 7), N-SHH+ODQ (n = 7), N-SHH+ODQ+Glibenclamide (n = 7). (C) Action potential duration at 95% of the repolarization (APD_{95},) in control (n = 7), SHH (n = 8), Control+glibenclamide (n = 7), N-SHH+glibenclamide (n = 8), N-SHH+L-NNA (n = 7), N-SHH+L-NNA+glibenclamide (n = 7), N-SHH+ODQ (n = 7), N-SHH+ODQ+Glibenclamide (n = 7). (D) The effect of glibenclamide (Glib) was further evaluated *in vivo* on the QT interval. Representative ECGs recorded in control (top), N-SHH (middle), and N-SHH+Glib (lower panel) treated animal. (E) Summary of the mean QTc value in each condition indicating the prevention of N-SHH effect in the presence of glibenclamide. (control n = 5, N-Shh n = 8, N-Shh+Glib n = 6, *, $p < 0.05$ compared to vehicle).

suggesting a production of NO. The NOS inhibitor N^{Ω}-nitro-L-arginine (L-NNA) prevented the effect of either N-SHH or MPs^{SHH+}. PI3K is known as a potential upstream NOS modulator[8]. SHH-induced NO production was inhibited in the presence of PI3K inhibitor, LY29402. Moreover, the effect of MPs^{SHH+} was prevented when cardiomyocytes were pre-incubated with cyclopamine. When cells were incubated with MPs lacking the SHH ligand (MPs^{SHH-},[10]), DAF fluorescence was comparable to non-treated cells. Altogether, this demonstrates that SHH pathway is present and functional in adult rat ventricular cardiomyocytes, and is functionally linked to NO production most likely through the PI3K/Akt upstream pathway.

SHH pathway modulates the action potential duration (APD). A reduction in QT interval without effect on heart rate and autonomic regulation should be linked to a reduction in APD. Indeed, isolated cardiomyocytes pre-incubated with N-SHH exhibited a shorter APD compared to non-treated cardiomyocytes as well as a significant hyperpolarized resting membrane potential (Figure 3A–C). The NO/cGMP pathway has been described to activate neuronal ATP-dependent potassium channel (K-ATP) in the absence of ATP depletion[15–17]. Interestingly, acute application of glibenclamide, the selective and specific blocker of K-ATP channels[18], prevented both APD reduction and resting membrane hyperpolarization induced by N-SHH although it had no effect in the absence of N-SHH (Figure 3A–C). Besides, blockade of NO and cGMP pathway by L-NNA and ODQ, respectively, blunted the effect of N-SHH. These experiments suggest the activation by SHH of the K-ATP current (I_{KATP}). The later effect of SHH was then confirmed *in vivo* in rats treated by iv-injection of glibenclamide (Figure 3D, E). Glibenclamide prevented the ability of N-SHH to reduce QTc as for cyclopamine.

Electrophysiological characterization of SHH-activated inward rectifying potassium current. Potassium currents were recorded prior to and after incubation with the blocker of K-ATP channels, glibenclamide[18]. The current difference reflecting I_{KATP} was measured at the end of the pulse to build the current-voltage relationship (Figure 4A, B). This current was absent in control conditions (Figure 4A, B, open symbols), but was induced by N-SHH (Figure 4A–B, closed symbols) and was inhibited by both L-NNA and ODQ (Figure 4C, D).

To corroborate these results, a numerical simulation was performed in the absence and the presence of an additional K^+ inward rectifying current adjusted to best mimic the experimental results of

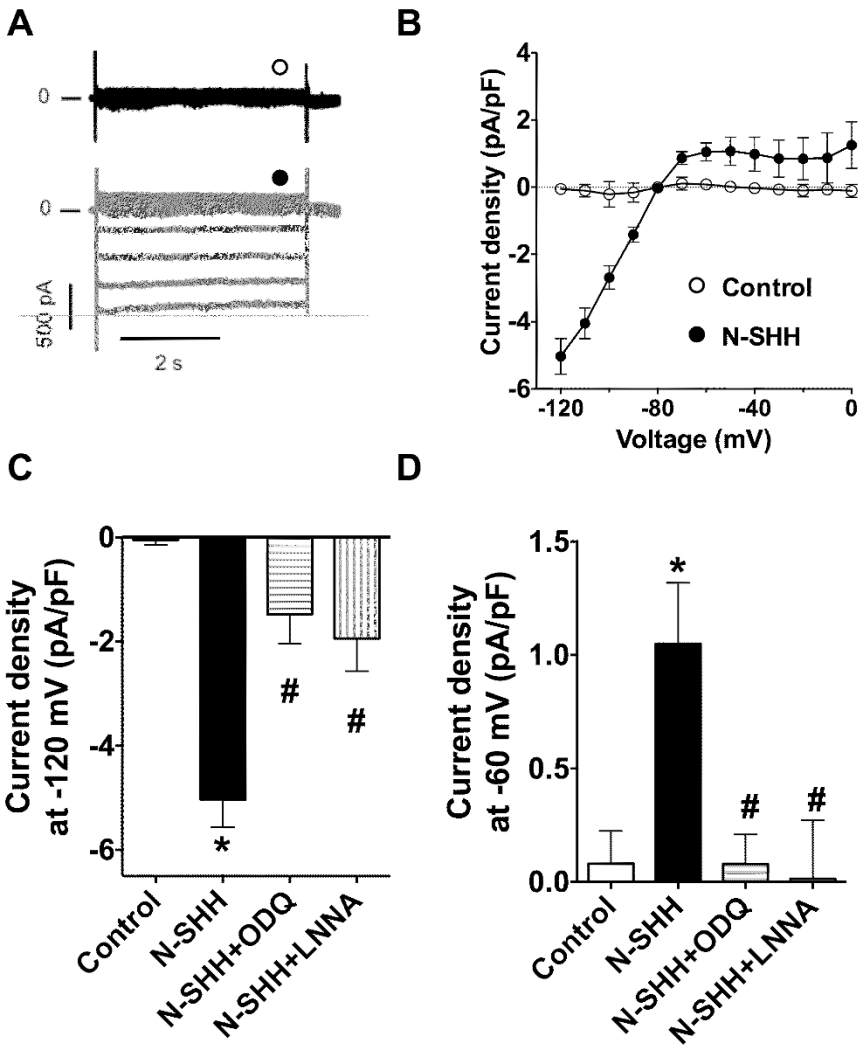

Figure 4 | SHH activates an inward rectifying potassium current glibenclamide-sensitive. (A) Family of current difference measured before and after application of glibenclamide from -120 mV to 0 mV in the absence (black traces) or in the presence of SHH (grey traces). (B) Average steady state currents expressed as current density are represented in control (n=8) and SHH (n=8). Similar experiments were also performed in the presence ODQ (n = 6) and L-NNA (n = 6). (C) The average current density at -120 mV. (D) The average current density at −60 mV. * and #, $p < 0.05$ compare to control *vs* N-SHH.

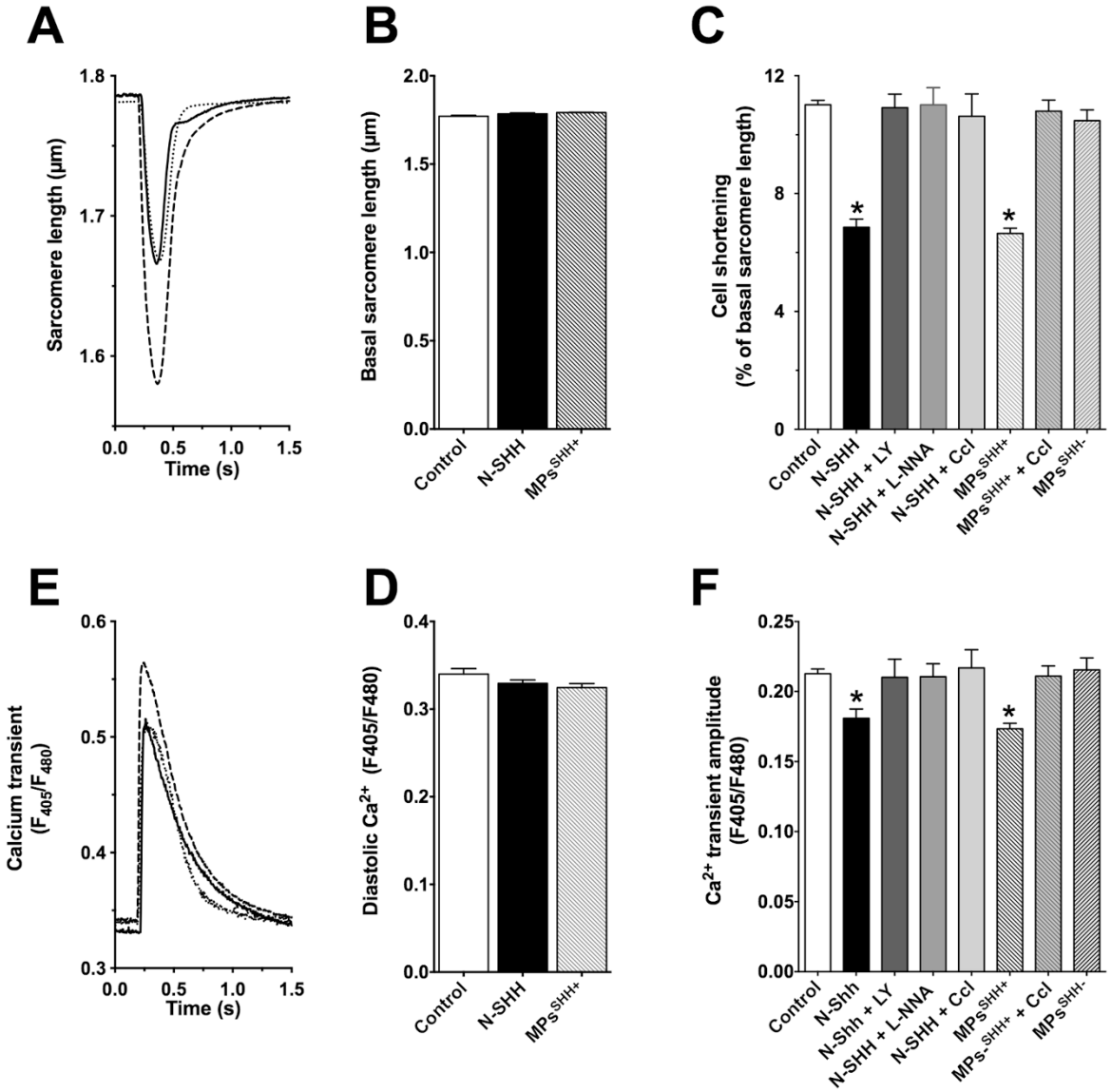

Figure 5 | SHH signal pathway inhibits excitation-contraction coupling of ventricular cardiomyocytes. (A) Representative time course of sarcomere length of control (dash line), N-SHH-treated (continuous line) and MPs^{SHH+}-treated cardiomyocytes (dot line) for 4 h. (B) Resting sarcomere length in control, N-SHH-treated and MPs^{SHH+}-treated cardiomyocytes. (C) Cell shortening (% of diastolic sarcomere length). (D) Representative time-course of Ca^{2+} transient (450/480 nm indo-1 fluorescence) of control (dashed line) cardiomyocytes and cardiomyocytes incubated with a recombinant SHH (N-SHH, continuous line) or MPs^{SHH+} (dotted line) for 4 h. (E) Diastolic Ca^{2+} levels in control, N-SHH-treated and MPs^{SHH+}-treated cardiomyocytes. (F) Ca^{2+} transient amplitude. All parameters were measured in control (n = 253), N-SHH-treated (n = 82) or MPs^{SHH+}-treated (n = 218) cardiomyocytes after incubation with phosphoinositide-3 kinase inhibitor, LY294002 (LY, 25 µM, n = 19), NOS inhibitor, N^{ω}-nitro-L-arginine (L-NNA, 100 µM, n = 19) and SHH pathway inhibitor, cyclopamine (Ccl, 30 µM, n = 17 with N-SHH and n = 75 with MPs^{SHH+}). Incubation with MPs lacking the SHH protein (MPs^{SHH-}, n = 25) did not modify the shortening or Ca^{2+} transient. Data are mean ± SEM, *, $p < 0.05$ compared to control.

the SHH-induced current (Figure S2A). Adding this inward rectifying K^+ conductance in the model reduced APD (Figure S2B). This was accompanied by a reduction in the Ca^{2+} transient (Figure S2D) and an increase in I_{CaL} amplitude (Figure S2C), but a reduction in the net amount of Ca^{2+} entering the cell (4.38 E^{10} vs 3.97 E^{10} Ca^{2+} ions in control and SHH respectively) due to shorter Ca^{2+} current and consequently reduced Ca^{2+}-induced Ca^{2+} release, as previously reported[19]. To validate the results generated by the numerical simulation, isolated cardiomyocytes were loaded with the Ca^{2+} probe indo-1 and paced at 0.5 Hz to evaluate in more details excitation-contraction coupling parameters (Figure 5). Sarcomere length variations and cytosolic Ca^{2+} were simultaneously recorded. Both N-SHH and MPs^{SHH+} reduced cell shortening triggered by the electrical stimulation (Figure 5A, E) without affecting the resting sarcomere length (Figure 5B). N-SHH or MPs^{SHH+} also significantly reduced Ca^{2+} transient amplitude (Figure 5C, F), while the diastolic Ca^{2+} remained statistically unchanged although slightly decreased (Figure 5D). We then evaluated the role of the signaling pathway activated by SHH in intact cardiomyocytes on both cell shortening (Figure 5E) and Ca^{2+} transient (Figure 5F) using specific inhibitors as described above for NO production (Figure 2). The reduction of cell shortening and Ca^{2+} transient amplitude induced by N-SHH was fully abolished in the presence of SHH pathway inhibitor cyclopamine, PI3K inhibitor LY249002 or the non-selective NOS inhibitor, L-NNA. The effect of N-SHH mimicked by MPs^{SHH+} was also blocked by cyclopamine while MPs^{SHH-} had no effect.

This reduction in cell shortening could be due either to the reduced Ca^{2+} transient amplitude and/or a direct action on the contractile machinery. Myofilament Ca^{2+} sensitivity was evaluated in Triton-X100 skinned cardiomyocytes[20]. As shown in Figure 6 (A, B), the

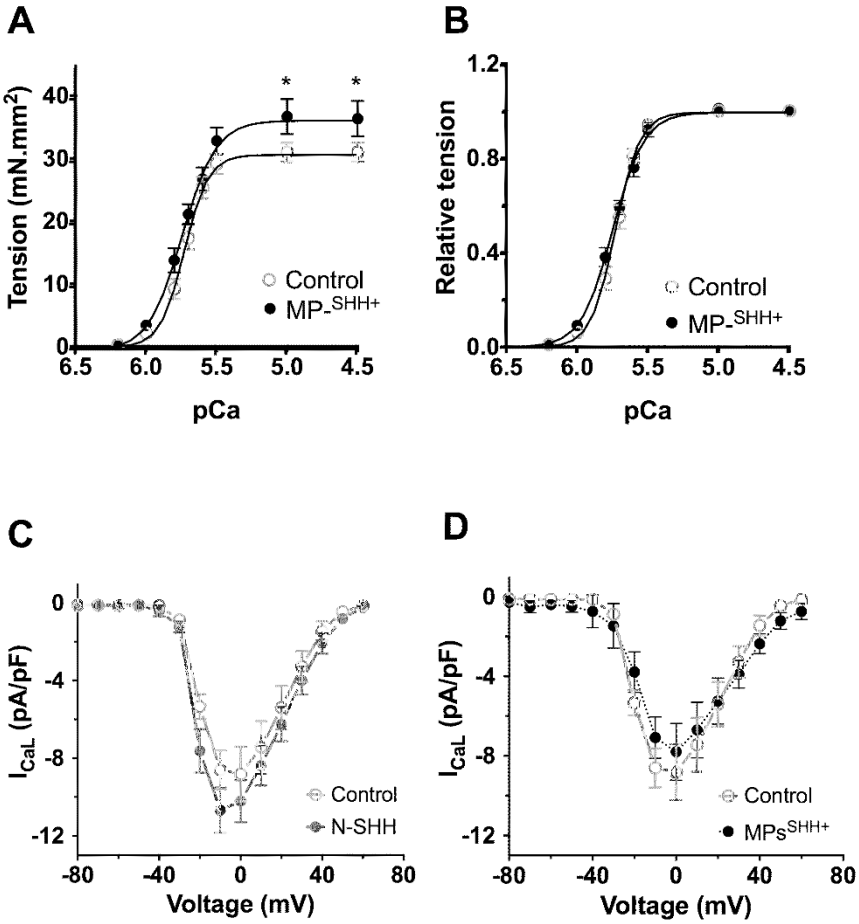

Figure 6 | SHH signal pathway on the cardiac excitation-contraction coupling. (A) Active tension of isometric permeabilized control and MPs^{SHH+}-treated cardiomyocytes (n = 12 in each condition). (B) Relative tension of isometric permeabilized control and MPs^{SHH+}-treated cardiomyocytes (n = 12 in each condition). (C) Effect of N-SHH on L type Ca^{2+} current density (I_{CaL} in pA/pF) as a function of membrane potential recorded in voltage-clamp in control (n = 7), recombinant SHH (N-SHH)-treated (N-SHH, n = 8) cardiomyocytes for 4 h. (D) Effect of MPs^{SHH+} on L type Ca^{2+} current density (I_{CaL} in pA/pF) as a function of membrane potential recorded in voltage-clamp in control (n = 7), Shh-harboring MPs (MPs^{SHH+})-treated (n = 8) cardiomyocytes for 4 h. * $p < 0.05$ compared to control.

tension-pCa relationships demonstrated a similar Ca^{2+} sensitization of the myofilament (pCa_{50} = 5.91 ± 0.03 and 5.87 ± 0.03 in control and MPs^{SHH+} conditions respectively, n = 12 cells per condition). A slight increase in maximal active tension was observed under MPs^{SHH+} treatment for pCa above 5.5. Altogether, these results support the hypothesis that the reduction in cell shortening by N-SHH and MPs^{SHH+} is the consequence of a reduced Ca^{2+} transient. We thus evaluated the effect of N-SHH and MPs^{SHH+} on the main cardiac Ca^{2+} release trigger, i.e. the L-type Ca^{2+} current (I_{CaL}, Figure 6 C, D) known to be modulated by NO[21]. In voltage-clamp condition, I_{CaL} was not directly affected by the SHH pathway. Finally, sarcoplasmic reticulum (SR) Ca^{2+} release measured as the peak Ca^{2+} transient measured after a rapid application of 10 mM caffeine was similar in non-treated cells and cells incubated with either N-SHH or MPs^{SHH+}, (F405/F480 ratio = 0.38 ± 0.02 (n=63), 0.37 ± 0.02 (n = 24) and 0.36 ± 0.02 (n = 36) respectively) suggesting that SHH pathway does not interfere directly with the SR compartment and SR dependent-Ca^{2+} release process.

Cardioprotective effect of SHH signaling pathway. The reperfusion injuries were histologically evaluated at 24 hours after reperfusion by measuring the infarcted area relative to the area at risk (Figure 7). Fifteen minutes prior to reperfusion, one group of rats received intraveinous (iv) injection N-SHH (25 $\mu g.kg^{-1}$), the second group received N-SHH and cyclopamine (N-SHH+Ccl, 30 μM) and the third one the vehicle (control). These experiments demonstrated a significant reduction of the infarcted area with N-SHH treatment. This N-SHH cardioprotective effect was prevented by cyclopamine (Figure 7A, B). Similar prevention was obtained by glibenclamide (Figure S3). These *in vivo* data demonstrate the potent role of SHH signaling pathway to protect the myocardium against reperfusion injuries after acute myocardial infarction (AMI). Considering that the cardioprotective effects are observed within a short time after reperfusion (i.e. <24 hours), it is unlikely that they are mediated by a neoangiogenesis and/or mobilization of progenitor cells[3,4]. We therefore hypothesized for another pleiotropic effect of SHH directly on the myocardial tissue.

We evaluated the ECG recorded before ischemia and during 24 hours after reperfusion in vigil animal by telemetry (Figure 8). After reperfusion, an enlargement of the QTc interval was observed. This effect was prevented in animals treated by a single injection of N-SHH prior to the reperfusion, without cardiodepressive effect on sinus rate. It is to note that the significance of this effect tends to disappear after 12 hours probably due to the elimination of the peptide and reversion of its effect (Figure 8A, 2B). When the animals were treated simultaneously with N-SHH and cyclopamine (N-SHH+Ccl), the prevention of QTc enlargement was abolished (Figure 8A, 2B). The beneficial effect of SHH was also prevented by glibenclamide (Figure S3). QT interval enlargement correlates *in vivo* with the occurrence of ventricular arrhythmias and is commonly used as a predictor for ventricular tachyarrhythmia and a risk

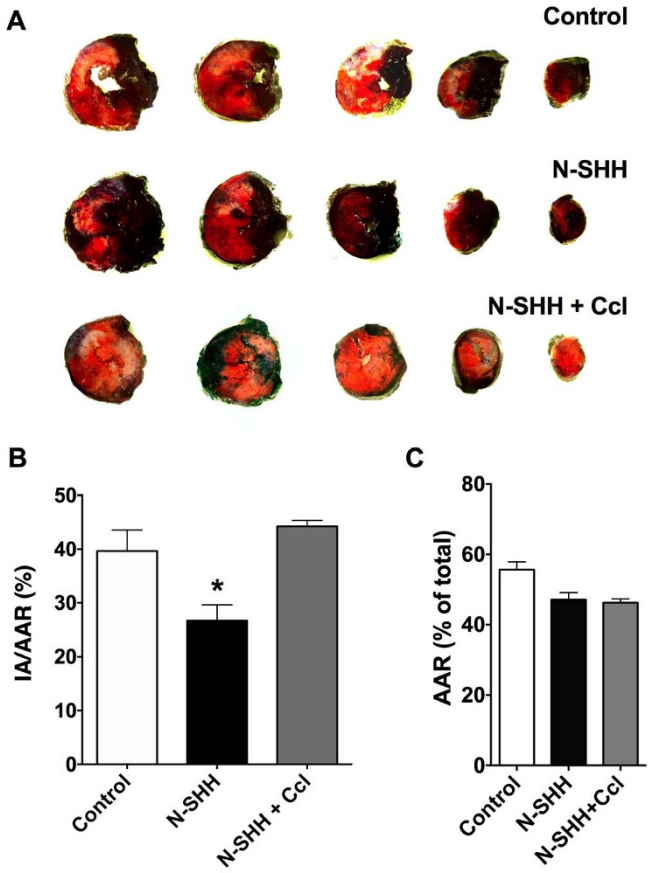

Figure 7 | Activation of the SHH pathway decreases the infarct size in a rat model of IR. (A) Representative sections (Upper) of TTC-stained hearts. (B) Quantification was analyzed by normalizing the infarct area (IA) to the area at risk (AAR). Treatment with N-SHH reduced infarct size after 24 h of reperfusion and this cardioprotective effect was prevented by cyclopamine. (C) No significant difference was observed in the total AAR between groups. Data are expressed as mean ± SEM (control n = 6, N-SHH n = 8, N-SHH + Ccl n = 6; * $p < 0.05$ *vs* control).

factor for sudden cardiac death[22,23]. Indeed, the treatment with N-SHH reduced significantly the number of ventricular arrhythmic events measured at the reperfusion (Figure 8C–D). This beneficial effect of SHH was abolished by cyclopamine and glibenclamide (Figure S3). Altogether, these experiments demonstrate a direct cardioprotective effect of SHH pathway on the myocardium involving an electrophysiological regulation.

Discussion

The present study demonstrates a novel cardioprotective effect of the morphogenetic SHH pathway in an *in vivo* model of IR in rats. It was previously reported that SHH signaling plays an important role in cardiomyogenesis during embryonic development[24]. The restitution of this signaling in adult rats after myocardial infarction improved cardiac reparation by enhancing neovascularization, reducing fibrosis and cardiac apoptosis[3]. It has been recently demonstrated that the stimulation of SHH at the surface membrane of cardiomyocytes was able to increase the expression of angiogenic cytokines mediating angiogenesis after myocardial infarction[6,7]. The present study demonstrates that SHH pathway activation prior to reperfusion by a single injection of either N-SHH or MPs^{SHH+} reduces infarct size and reperfusion arrhythmias *via* a prevention of QT enlargement. Prolongation of QT interval has been associated with an increased risk of sudden cardiac death after AMI in patients both in short and long term[25]. It is now admitted that reduction of QT interval and QT interval variability after reperfusion is beneficial and indicative of a successful reperfusion in patients undergoing primary percutaneous coronary angioplasty[26].

The stimulation of SHH pathway both by incubation with N-SHH recombinant protein and shed membrane MPs^{SHH+10} has an acute physiological effect on isolated cardiomyocytes. These effects were abolished by cyclopamine, a specific inhibitor of the SHH pathway which binds to Smo[27]. Moreover, the incubation of isolated cardiomyocytes with apoptotic T lymphocyte-derived MPs (MPs^{SHH-}) lacking SHH protein[10] had no effect on cardiomyocytes. These data provide convincing evidence of the potential role of SHH signaling pathway in adult cardiac tissue. Our results confirm that SHH either as a recombinant protein or carried by MPs is able to induce NO generation via SHH/PI3-K/Akt/NOS pathway with physiological consequences in adult cardiomyocytes as reported in both cultured endothelial cells and isolated coronary arteries[8]. The physiological effects of NO on cardiac function are however still controversial with positive[28] or negative[29] influence on cardiomyocyte contractility. The final outcome seems to depend on NO concentration, level of adrenergic stimulation, oxidative status and the specific NOS isoform activated[21]. In our experiments, the enhanced SHH-induced NOS activation was associated with reduced cardiomyocyte Ca^{2+} transient and reduced shortening. The mechanisms generally responsible for the NO-induced reduction of cardiac contractility are still not completely elucidated. Some studies attributed the reduction to attenuated Ca^{2+} mobilization[30], while others suggest reduced Ca^{2+} sensitivity due to troponin I phosphorylation[31]. However, we have not observed any alterations of sarcomeric machinery. In our experiments, we have not observed any alteration of the Ca^{2+} transient caused by caffeine-induced Ca^{2+} release from the SR either, suggesting a preserved SR Ca^{2+} load and SR function. NO has multiple ionic target in cardiomyocytes to modulate action potential waveform (for review[18]). However in the present study the elevation of NO has no effect in the depolarization phase of the AP as well as the early phase of the repolarization and I_{CaL}.

We demonstrate here that SHH-induced NO formation specifically reduces APD through the activation of an inward rectifying current with electrophysiological and pharmacological properties of the I_{KATP}. This decreased the amount of Ca^{2+} entering the cell through the L-type Ca^{2+} channel and consequently reduces both Ca^{2+} transient and sarcomere length shortening of isolated cardiomyocytes. Together, these data demonstrate the physiological and pathophysiological implication of I_{KATP} independently of metabolic injury or ATP depletion. This specific effect also suggests a close compartmentation and functional association between SHH-mediated NO production and IK_{ATP} activation rendering this pathway highly specific. This contrasts however with previous reports concluding that, in ventricular myocytes, NO donors are unable to activate IK_{ATP} directly but it potentiates the same current[32] by a mechanism involving a NO/cGMP/PKG dependent phosphorylation[33].

Therefore, SHH activates a glibenclamide sensitive current most likely carried out by a Kir 6.x/SURx K-ATP channel[18,34]. Although it is one of the most abundantly expressed plasma membrane channels in cardiomyocytes[34], it is thought to play no role under normal condition. Nevertheless and due to its abundance, 1% of channel activation may shorten the APD by 50%[35]. Its role in cardiac physiology and/or pathophysiology remains, besides drastic energetic impairments, poorly elucidated. Recently, it has been demonstrated that NO/cGMP pathway could directly activate the neuronal K-ATP[16,17]. This result is in complete agreement with our data, which strongly supports the hypothesis of I_{KATP} activation by SHH signaling *via* NO/cGMP pathway. This would provide evidences for a potentially new regulatory pathway of this specific channel in cardiomyocytes.

The SHH-induced reduction in APD prevents the occurrence of arrhythmic events and reduces both Ca^{2+} entry and release that may prevent deleterious Ca^{2+} overload at the onset of myocardial reper-

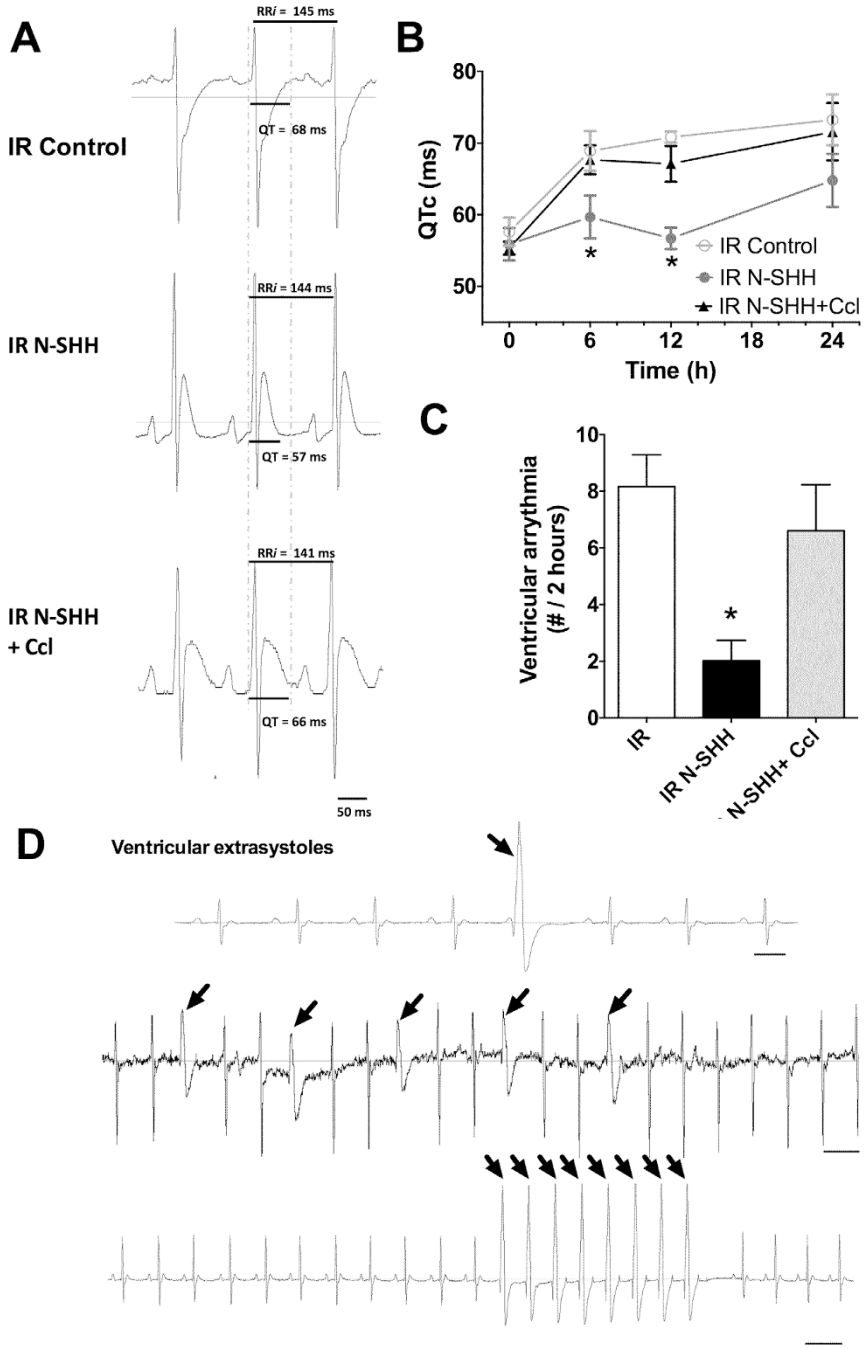

Figure 8 | Activation of SHH signaling improves ventricular repolarization after ischemia-reperfusion. (A) ECGs were acquired over 24 h of reperfusion following 30min ischemia, in animal treated (i.v. injected 15 min prior reperfusion) either with the vehicle, recombinant N-SHH, or N-SHH + Cyclopamine (Ccl). Typical ECGs at 6 hours post reperfusion exhibited an enlargement of QT interval corrected for heart rate (QTc). (B) Time course of QTc variation is summarized in the 3 different experimental conditions. (C) Summarizes the number of arrhythmias recorded over a period of 2 hours following reperfusion showing a reduction of ventricular arrhythmia when SHH signaling pathway is activated. (D) Three representative patterns of ventricular arrhythmias (indicated by arrows) recorded after reperfusion in animals treated with the vehicle only (control). (control n = 6, N-SHH n = 8, N-SHH + Ccl n = 6; * $p < 0.05$).

fusion[36]. However, the local activation of K-ATP channels during AMI[37] might result in an increased concentration of potassium leading to spatial heterogeneities in excitability, conduction, refractoriness favoring and in turn associated with arrhythmogenic potential. This is supported by the observation that inhibiting specifically K-ATP channel during coronary occlusion reduces mortality and ischemia-associated electrocardiographic changes in a pig model[38]. This is in apparent contradiction with our observation demonstrating the beneficial effect of the activation of inward potassium current. However in pathophysiological situation, I_{KATP} channels activate, only locally (i.e. in the infarcted area) and only during ATP depletion. Here we provide evidence that such current can be activated in all the myocardium territory independently of the ATP level. Therefore, this should reduce the heterogeneity of repolarization induced by the ischemic phase and associated reentry-induced ventricular tachyarrhythmia, preserve cellular energy balance at varying workloads and limit overall Ca^{2+} overload at the reperfusion, which might also be highly beneficial for the myocardium both in term of arrhythmic events as

well as reperfusion injuries[36]. A direct pharmacological strategy using either direct or indirect K-ATP activator has been considered for a long time for cardioprotection[39]. Our present data reinforced the interest for addressing this particular channel in cardioprotection.

In conclusion, we demonstrate the physiological and pathophysiological importance and a novel regulatory role of the SHH pathway in adult cardiomyocytes. We have previously shown that SHH pathway activation stimulates the release of endothelial NO and correct endothelial dysfunction subsequent to IR[8], and hypertension[40]. Moreover, SHH improves neovascularization in hindlimb ischemia[6,9]. The morphogen SHH holds great promise for regeneration of tissues suffering after ischemic injury by recruiting progenitor cells[5,41]. The present study shows for the first time a direct protective effect of SHH pathway against AMI on cardiac tissue. All together these pleiotropic effects of SHH participate in cardioprotection by acting simultaneously on different targets.

Methods

Ethics Statement. All experiments were conducted in accordance with relevant guidelines and regulations, conformed to European Parliament Directive 2010/63/EU and the Guide for the Care and Use of Laboratory Animals of the NIH (No. 85–23, revised 1996). The protocols were approved by the local ethics committee rules (CEEA-LR-12079).

Recording and Analysis of ECG. ECGs were recorded by using a signal transmitter (TAF40-Physiotel®)-receiver (RPC-1) connected to a data acquisition system (Ponemah Physiology Platform, DSI, Sat Paul, USA)) as previously reported[42] The data were collected continuously over 24 hours (sampling rate of 1 kHz). Digital recordings were analyzed offline with ECG-auto software (ver 1.5.12.22, EMKA Technologies). ECG signals were digitally filtered between 0.1 and 100 Hz and analyzed manually to detect arrhythmias and measure QT interval. T-wave calculations were made on the basis of the repolarization wave that followed the QRS complex. The method used to define the QT duration was to consider the QT interval between the first deviation from an isoelectric PR interval until the final return of the ventricular repolarization to the isoelectric TP baseline. This was included in the measure the low-amplitude portion of the T-wave and allowed a complete ventricular repolarization of ventricles. The RR and the QT duration over a large period of ECG were determined "beat-by-beat" to limit a possible bias due to a subjective "peak-out" of QRST complexes and variable shape of T wave. Thus, at least 5000 QRST complexes were analyzed. ECG signal was analyzed by using software that recognized the shape of the tracing and placed pre-calibrated gauges after having well-defined isoelectric baseline. The operator manually validated the QT determination or excluded it if a doubt existed (noise or movement artifact for example). The time interval between 2 consecutive R deflections was then automatically calculated and recorded with the QT interval. By this common method the QT ranges in literature from 65 to 85 ms in control rats with an RR interval comprised between 150 to 180 ms.

Rat model of Ishemia-reperfusion. Eight-week-old Wistar Kyoto rats (Janvier) were anesthetized with pentobarbital (Abbott; 40 mg/kg, intraperitonaly (i.p.)), and ventilated 60 times per min with a volume-cycled respirator. The left coronary artery was ligated at 1–2 mm from its origin (5-0 silk suture; Autosuture; Tyco Healthcare). After 15 min of ligation, animals were randomly given vehicle (0.9% saline), N-SHH (i.v., 0.4 μg/mL in 0.9% saline), or MPs^{SHH+} (i.v., 10 μg/mL in 0.9% saline). After 30 min of occlusion, the ligation was removed and the left coronary artery was reperfused. Rats were randomly assigned to study groups according to the duration of left coronary reperfusion Sham-operated animals were subjected to the same surgical procedure, but the ligation remained untied.

Statistics. Presented numerical data are Mean ± standard error of mean (SEM). Results were considered significant if $p < 0.05$, with one-way, two-tailed Analysis of Variance (ANOVA) with Bonferroni post-test.

Further details on methods are included in Supplementary material online.

1. Ericson, J., Morton, S., Kawakami, A., Roelink, H. & Jessell, T. M. Two critical periods of Sonic Hedgehog signaling required for the specification of motor neuron identity. *Cell* **87**, 661–673 (1996).
2. Levin, M., Johnson, R. L., Stern, C. D., Kuehn, M. & Tabin, C. A molecular pathway determining left-right asymmetry in chick embryogenesis. *Cell* **82**, 803–814 (1995).
3. Kusano, K. F. *et al.* Sonic hedgehog myocardial gene therapy: tissue repair through transient reconstitution of embryonic signaling. *Nat Med* **11**, 1197–1204 (2005).
4. Pola, R. *et al.* The morphogen Sonic hedgehog is an indirect angiogenic agent upregulating two families of angiogenic growth factors. *Nat Med* **7**, 706–711 (2001).
5. Lavine, K. J., Kovacs, A. & Ornitz, D. M. Hedgehog signaling is critical for maintenance of the adult coronary vasculature in mice. *J Clin Invest* **118**, 2404–2414 (2008).
6. Renault, M. A. *et al.* Gli3 regulation of myogenesis is necessary for ischemia-induced angiogenesis. *Circ Res* **113**, 1148–1158 (2013).
7. Ueda, K. *et al.* Sonic hedgehog is a critical mediator of erythropoietin-induced cardiac protection in mice. *J Clin Invest* **120**, 2016–2029 (2010).
8. Agouni, A. *et al.* Sonic hedgehog carried by microparticles corrects endothelial injury through nitric oxide release. *Faseb J* **21**, 2735–2741 (2007).
9. Benameur, T., Soleti, R., Porro, C., Andriantsitohaina, R. & Martinez, M. C. Microparticles carrying Sonic hedgehog favor neovascularization through the activation of nitric oxide pathway in mice. *PLoS One* **5**, e12688 (2010).
10. Martinez, M. C. *et al.* Transfer of differentiation signal by membrane microvesicles harboring hedgehog morphogens. *Blood* **108**, 3012–3020 (2006).
11. Marigo, V., Davey, R. A., Zuo, Y., Cunningham, J. M. & Tabin, C. J. Biochemical evidence that patched is the Hedgehog receptor. *Nature* **384**, 176–179 (1996).
12. Denef, N., Neubuser, D., Perez, L. & Cohen, S. M. Hedgehog induces opposite changes in turnover and subcellular localization of patched and smoothened. *Cell* **102**, 521–531 (2000).
13. Riobo, N. A., Lu, K., Ai, X., Haines, G. M. & Emerson, C. P. Jr. Phosphoinositide 3-kinase and Akt are essential for Sonic Hedgehog signaling. *Proc Natl Acad Sci U S A* **103**, 4505–4510 (2006).
14. Mutoh, A., Isshiki, M. & Fujita, T. Aldosterone enhances ligand-stimulated nitric oxide production in endothelial cells. *Hypertens Res* **31**, 1811–1820 (2008).
15. Chai, Y. & Lin, Y. F. Dual regulation of the ATP-sensitive potassium channel by activation of cGMP-dependent protein kinase. *Pflugers Arch* **456**, 897–915 (2008).
16. Chai, Y. & Lin, Y. F. Stimulation of neuronal KATP channels by cGMP-dependent protein kinase: involvement of ROS and 5-hydroxydecanoate-sensitive factors in signal transduction. *Am J Physiol Cell Physiol* **298**, C875–892 (2010).
17. Galdino, G. S., Cortes, S. F., Duarte, I. D. & Perez, A. C. Involvement of the nitric oxide/(C)GMP/K(ATP) pathway in antinociception induced by exercise in rats. *Life Sci* **86**, 505–509 (2010).
18. Tamargo, J., Caballero, R., Gomez, R., Valenzuela, C. & Delpon, E. Pharmacology of cardiac potassium channels. *Cardiovasc Res* **62**, 9–33 (2004).
19. Bouchard, R. A., Clark, R. B. & Giles, W. R. Effects of action potential duration on excitation-contraction coupling in rat ventricular myocytes. Action potential voltage-clamp measurements. *Circ Res* **76**, 790–801 (1995).
20. Cazorla, O., Szilagyi, S., Le Guennec, J. Y., Vassort, G. & Lacampagne, A. Transmural stretch-dependent regulation of contractile properties in rat heart and its alteration after myocardial infarction. *Faseb J* **19**, 88–90 (2005).
21. Hare, J. M. Nitric oxide and excitation-contraction coupling. *J Mol Cell Cardiol* **35**, 719–729 (2003).
22. Antzelevitch, C., Shimizu, W., Yan, G. X. & Sicouri, S. Cellular basis for QT dispersion. *Journal of electrocardiology* **30 Suppl**, 168–175 (1998).
23. Hlaing, T., DiMino, T., Kowey, P. R. & Yan, G. X. ECG repolarization waves: their genesis and clinical implications. *Annals of noninvasive electrocardiology : the official journal of the International Society for Holter and Noninvasive Electrocardiology, Inc* **10**, 211–223 (2005).
24. Gianakopoulos, P. J. & Skerjanc, I. S. Hedgehog signaling induces cardiomyogenesis in P19 cells. *J Biol Chem* **280**, 21022–21028 (2005).
25. Schwartz, P. J. & Wolf, S. QT interval prolongation as predictor of sudden death in patients with myocardial infarction. *Circulation* **57**, 1074–1077 (1978).
26. Bonnemeier, H., Hartmann, F., Wiegand, U. K., Bode, F., Katus, H. A. & Richardt, G. Course and prognostic implications of QT interval and QT interval variability after primary coronary angioplasty in acute myocardial infarction. *Journal of the American College of Cardiology* **37**, 44–50 (2001).
27. Taipale, J. *et al.* Effects of oncogenic mutations in Smoothened and Patched can be reversed by cyclopamine. *Nature* **406**, 1005–1009 (2000).
28. Kojda, G., Kottenberg, K., Nix, P., Schluter, K. D., Piper, H. M. & Noack, E. Low increase in cGMP induced by organic nitrates and nitrovasodilators improves contractile response of rat ventricular myocytes. *Circ Res* **78**, 91–101 (1996).
29. Brady, A. J., Warren, J. B., Poole-Wilson, P. A., Williams, T. J. & Harding, S. E. Nitric oxide attenuates cardiac myocyte contraction. *Am J Physiol* **265**, H176–182 (1993).
30. Ziolo, M. T., Katoh, H. & Bers, D. M. Positive and negative effects of nitric oxide on Ca(2+) sparks: influence of beta-adrenergic stimulation. *Am J Physiol Heart Circ Physiol* **281**, H2295–2303 (2001).
31. Layland, J., Li, J. M. & Shah, A. M. Role of cyclic GMP-dependent protein kinase in the contractile response to exogenous nitric oxide in rat cardiac myocytes. *J Physiol* **540**, 457–467 (2002).
32. Shinbo, A. & Iijima, T. Potentiation by nitric oxide of the ATP-sensitive K+ current induced by K+ channel openers in guinea-pig ventricular cells. *British journal of pharmacology* **120**, 1568–1574 (1997).
33. Han, J. & Kim, N., Joo, H., Kim, E. & Earm, Y. E. ATP-sensitive K(+) channel activation by nitric oxide and protein kinase G in rabbit ventricular myocytes. *Am J Physiol Heart Circ Physiol* **283**, H1545–1554 (2002).
34. Flagg, T. P., Enkvetchakul, D., Koster, J. C. & Nichols, C. G. Muscle KATP channels: recent insights to energy sensing and myoprotection. *Physiol Rev* **90**, 799–829 (2010).
35. Zhang, H., Flagg, T. P. & Nichols, C. G. Cardiac sarcolemmal K(ATP) channels: Latest twists in a questing tale! *J Mol Cell Cardiol* **48**, 71–75 (2010).

36. Fauconnier, J., Roberge, S. & Saint, N., Lacampagne, A. Type 2 ryanodine receptor: a novel therapeutic target in myocardial ischemia/reperfusion. *Pharmacology & therapeutics* **138**, 323–332 (2013).
37. Noma, A. ATP-regulated K+ channels in cardiac muscle. *Nature* **305**, 147–148 (1983).
38. Wirth, K. J., Rosenstein, B., Uhde, J., Englert, H. C., Busch, A. E. & Scholkens, B. A. ATP-sensitive potassium channel blocker HMR 1883 reduces mortality and ischemia-associated electrocardiographic changes in pigs with coronary occlusion. *The Journal of pharmacology and experimental therapeutics* **291**, 474–481 (1999).
39. Kane, G. C., Liu, X. K., Yamada, S. Olson, T. M. & Terzic, A. Cardiac KATP channels in health and disease. *J Mol Cell Cardiol* **38**, 937–943 (2005).
40. Marrachelli, V. G. *et al.* Sonic hedgehog carried by microparticles corrects angiotensin II-induced hypertension and endothelial dysfunction in mice. *PLoS One* **8**, e72861 (2013).
41. Johnson, N. R. & Wang, Y. Controlled delivery of sonic hedgehog morphogen and its potential for cardiac repair. *PLoS One* **8**, e63075 (2013).
42. Fauconnier, J. *et al.* Ryanodine receptor leak mediated by caspase-8 activation leads to left ventricular injury after myocardial ischemia-reperfusion. *Proc Natl Acad Sci U S A* **108**, 13258–13263 (2011).

Acknowledgments

This work was supported by the "Institut de la Santé et de la Recherche Médicale" (Inserm), "Région Languedoc Roussillon". "Région Pays de la Loire (CIMATH-2)". The funders had no role in study design, data collection and analysis, or preparation of the manuscript. AL, JF, JT, MCM, OC are scientists from « Centre National de la Recherche Scientifique » (CNRS).

Author contributions

LP, RA, MCM and AL. were involved in the conception and design of the studies. LP, JF, OC, JT, RS, BV, AO, MB, PB, JYL were involved in the collection, analysis and interpretation of the data. LP, RA, MCM, FR and AL were mainly responsible for drafting the article and critical input was obtained from all other authors. All authors approved the final version of the manuscript.

Additional information

Supplementary information accompanies this paper at http://www.nature.com/scientificreports

Competing financial interests: The authors declare no competing financial interests.

How to cite this article: Paulis, L. *et al.* Activation of Sonic hedgehog signaling in ventricular cardiomyocytes exerts cardioprotection against ischemia reperfusion injuries. *Sci. Rep.* **5**, 7983; DOI:10.1038/srep07983 (2015).